ISBN: 978-3-95450-184-7 doi:10.18429/JACoW-IPAC2018-TUPAL035

3D BEAM DYNAMICS MODELING OF MEBT FOR THE NEW LANSCE RFQ INJECTOR

S.S. Kurennoy, LANL, Los Alamos, NM 87545, USA

Abstract

The new RFQ-based proton injector at LANSCE requires a specialized medium-energy beam transfer (MEBT) after the RFQ at 750 keV due to a following long (~3 m) existing common transfer line that also serves for transporting negative-ion beams to the DTL entrance. The horizontal space for MEBT elements is limited because two beam lines merge at 18-degree angle. The MEBT design developed with envelope codes includes two compact quarter-wave RF bunchers and four short quadrupoles with steerers, all within the length of about 1 m. The beam size in the MEBT is large, comparable to the beam-pipe aperture, hence non-linear 3D field effects at large radii become important. Using CST Studio codes, we calculate buncher RF fields and quadrupole magnetic fields and use them to perform particle-in-cell beam dynamics modeling of MEBT with realistic beam distributions from the RFQ. Our results indicate a significant emittance growth not predicted by standard beam dynamics codes. Its origin was traced mainly to the quadrupole edge fields. Quadrupole design modifications are proposed to improve the MEBT performance.

INTRODUCTION

A modern front end for the LANSCE linac is under development: the aging Cockcroft-Walton based injectors will be replaced by modern RFQ-based ones [1]. Now two lines, one for H^+ (proton) and the other for H^- ions, produce 750-keV beams that merge into a common transport, which goes to the entrance of the first DTL tank. The proton injector will be upgraded first, but the existing common transport line for different beam species creates significant constrains for the injector line design. The first challenge is a very long distance from the proton RFQ exit to the DTL entrance, more than 4 m. Second, because the two beam lines merge at 18-degree angle, the horizontal space for proton-line elements is limited by the existing hardware near the merging area. Therefore, a specialized medium-energy beam transfer (MEBT) after the new proton RFQ at 750 keV was developed [2] with envelope codes, and the beam dynamics in MEBT was modeled using Parmila [3]. The MEBT shapes the RFQ output beam to transfer it through the long existing common transport to the DTL with minimal losses. The MEBT includes four electromagnetic (EM) quadrupole magnets and two buncher cavities [2], all within about 0.9 m along the beam line, followed by a 0.5-m long drift to the merging point of the common transport line, which continues for about 2.7 m to the DTL entrance. The beam pipe in the proton injector line has inner diameter (ID) 1.875" (aperture radius $a = 2.38125$ cm) and outer diameter 2"; the pipe wall thickness is 1/16" (≈ 0.159 cm).

The proton beam size in the MEBT is large, comparable to the beam-pipe aperture, hence one can expect that non-linear 3D field effects at large radii become important. Using CST Studio codes [4], we calculate buncher RF fields and quadrupole and steerer magnetic fields, and then apply them to perform particle-in-cell (PIC) beam dynamics modeling of MEBT with realistic beam distributions from the RFQ.

MEBT ELEMENTS

The main MEBT elements are two compact quarter-wave (QW, $\lambda/4$) 201.25-MHz RF cavity bunchers and four short EM quadrupole magnets with additional windings for beam steering; their models are shown in Fig. 1. Both types of elements have a very small footprint on the beamline, below 8 cm. The QW buncher is a coaxial resonator with two gaps separated by distance $\beta\lambda/2 = 2.98$ cm for $\beta = 0.04$. The short quads with steerers were originally designed for APT and later modified for SNS, see in [5].

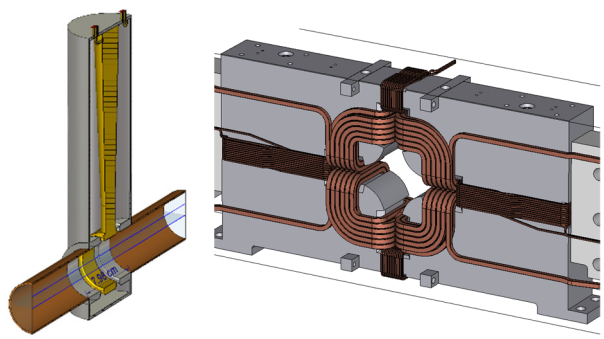

Figure 1: MEBT element models: QW buncher (left, cut) and EM quad with two pairs of steerers (right).

The bunchers (B) and quadrupoles (Q) are arranged in the MEBT in the following order: Q_1, B_1, Q_2, Q_3, Q_4, and B_2. The buncher and quadrupole parameters and fields were calculated using CST MicroWave (MWS) and EM (EMS) Studios, see details in [5]. The maximal effective voltage of QW buncher required by the design [2] is $V_{\text{eff}} =$ 25 kV (12.5 kV per gap). The quad effective length is 7.6 cm with gradients G from 7.1 to 10.8 T/m. Using the CST-calculated 3D RF and magnetic fields, we proceed with beam dynamics modeling of the MEBT using particle-in-cell (PIC) solver in CST Particle Studio (PS).

BEAM DYNAMICS IN MEBT

Initial Beam Distributions

For initial beam distributions in MEBT PIC modeling we use two realistic distributions for the proton beam at the RFQ exit from previous macro-particle simulations. In

ISBN: 978-3-95450-184-7 doi:10.18429/JACoW-IPAC2018-TUPAL035

both cases, a 24-mA current beam was simulated with 10K particles at the RFQ entrance. One output distribution is from ParmteqM runs (provided by L. Rybarcyk), converted into PS input format; another one is from our PS simulations [6] that used MWS-calculated RFQ fields. Some parameters of these initial beam distributions are summarized in Table 1.

Table 1: Initial Beam Distribution Parameters

Parameter, units	ParmteqM	PS
Proton beam current, mA	23.5	22.6
Number of macro-particles N	9788	9397
Average particle energy, keV	750	754
Norm. rms emittance $\varepsilon_{x,}$ π μm	0.22	0.25
Norm. rms emittance $\varepsilon_{y,}$ π μm	0.22	0.25
Rms longit. emittance $\varepsilon_{z,}$ π μm	0.28	0.35

The average transverse coordinates and angles for the ParmteqM distribution are small, below 0.01 mm and 1 mrad, but for the PS one they are larger: -0.16 & 0.43 mm, -6.7 & 6.2 mrad in x and y, respectively. Note that these two distributions are recorded at two different locations: the ParmteqM output is at the exit inner RF wall of the RFQ box, while the PS results are in the RFQ exit beam pipe, in the transverse plane 4.5 cm downstream. Therefore, we make two PS models: both end at 15 cm after the B_2 center, in the field-free region, but have different total lengths, 106.17 cm and 101.67 cm.

PIC Simulations

PS models include a cylindrical beam pipe and imported properly scaled buncher RF fields and magnet fields. The quad magnetic fields correspond to the design gradients, the buncher effective voltages are 25 kV in B_1 and 18 kV in B_2 [2]. The buncher RF phases are adjusted such that the bunch center arrives at B_1 center at 180°, which provides bunching in 2-gap cavities, and at 152° in B_2 for ParmteqM case. For PS input, the beam energy is corrected (-4 keV) in B_1, so the RF phases are 167° in B_1 and 152° in B_2.

After that the beam dynamics is modeled with the CST PS PIC solver by running the initial beam through the MEBT fields. The particle parameters are recorded using 2D plane particle monitors located along the MEBT at the centers of all elements, in the exit plane, and ±5 cm from both bunchers. For initial PS runs, no steering was applied. For the well-centered ParmteqM initial distribution, the beam center is just slightly off axis (within 2 mm). The PS distribution has noticeable initial average angles, and the off-axis deviations can be as large as 5 mm, with tilt angles more than 15 mrad without steering. Particle losses are also significant in the PS-input case, 9%, compared to 2.6% for the ParmteqM input. The particles are lost mostly between Q_2 and Q_4. They are scraped by the chamber wall as the beam size increases after B_1 and the beam is steered off axis by the quad fields. So some beam steering is necessary.

We add the CST-calculated steerer fields and adjust their magnitude to minimize the beam-center displacements along the MEBT. One should note that the quad steerers, cf. Fig. 1, introduce some x-y coupling: they deflect off-axis particles not only in the desired direction (e.g. in x) but also slightly in the transverse direction (y), see in [5]. The steering tuning is easy for the ParmteqM input beam: with low steering currents one can keep all displacements within a fraction of 1mm and all tilts below 1 mrad. For the PS input beam, which has significant initial tilt angles, higher steering currents are required to keep the deviations below 1 mm. With the steering implemented, the particle losses are reduced: for ParmteqM input – from 2.6% to 2.1%, and significantly for PS input – from 9% down to 3.2%. However, the beam transverse emittances still increase significantly even for the steered beams, see Fig. 2, where the normalized rms transverse emittances and the longitudinal rms emittance along the MEBT are plotted for ParmteqM input distribution. The horizontal emittance ε_x increases by about a factor of ~3 and the vertical ε_y grows by a factor of <2. The horizontal emittance jumps after the quad Q_3, while the vertical one starts to increase after Q_2. For the PS input, the emittance behavior is similar. The longitudinal emittance increases by about 35% for both distributions, mainly in the second buncher, B_2.

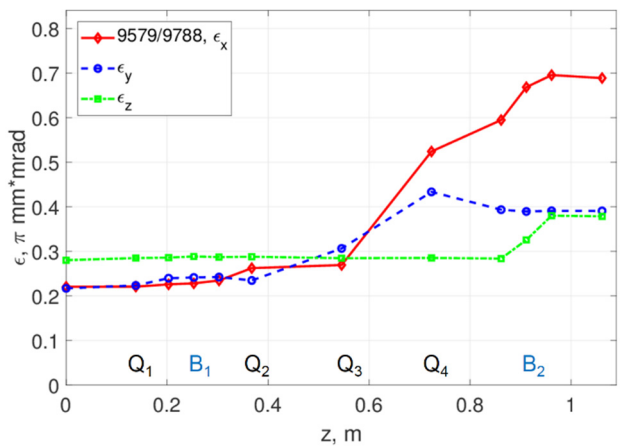

Figure 2: Evolution of beam emittances along the MEBT.

Beam Dynamics Results and Discussion

Such large emittance increases are unexpected: they are much higher than the predictions in the design [2], ~30% for transverse emittances. However, the longitudinal emittance increases 36%, well below 128% in [2]. We search for the reasons of the transverse emittance growth and how it can be mitigated. There are differences between Trace/Parmila and CST models. First, Parmila uses ideal hard-edge (HE) quadrupole fields. Second, the bunchers in Parmila are modeled as zero-length single gaps, with longitudinal and transverse kicks to the passing particles that depend on the particle radial position. With ParmteqM input, we study various MEBT configurations: substituting CST-computed quad fields (EM) by ideal quadrupole fields (HE), turning bunchers on and off, etc. Our PIC simulation results are summarized in Table 2.

ISBN: 978-3-95450-184-7 doi:10.18429/JACoW-IPAC2018-TUPAL035

Table 2: Parameter Changes vs. MEBT Configuration

Case	B	Q	S	N/N_0	$\varepsilon_x/\varepsilon_{x0}$	$\varepsilon_y/\varepsilon_{y0}$	$\varepsilon_z/\varepsilon_{z0}$
1	on	EM	on	0.979	3.14	1.77	1.36
2	on	HE	off	0.991	1.68	1.14	1.18
3	off	HE	off	0.999	1.23	1.14	1.0
4	off	EM	off	0.995	2.23	1.50	1.0
5	off	EM	on	0.996	2.00	1.55	1.0
6	1g	HE	off	0.986	1.91	1.18	1.29

The notations in Table 2 are B for bunchers, Q for quads, and S for steerers; N is the number of macro-particles. The cases correspond to the following configurations: 1. Real MEBT with CST fields; 2. Ideal HE quads; 3. Bunchers off with HE quads; 4. Same with EM quads; 5. Case 4 with steering; 6. QW buncher RF fields are substituted by RF fields of 1-gap re-entrant cavity, with HE quads. One can see that steerer effects are small (4 vs. 5). HE quads reduce the emittance growth noticeably (2 vs. 1). QW bunchers are slightly better than 1-gap ones (2 vs. 6). Cases 3-5 are for comparison only since there is no bunching. In case 3, the beam is just transferred through; transverse emittances increase by 15-20% due to space charge. The buncher fields mostly affect the horizontal emittance (2 vs. 3), increasing it by a factor of 1.5 on top of the space charge increase. With bunchers off, the EM quad field increase the horizontal emittance by a factor of ~1.75 above the space charge, cf. 3, 4, and 5. The combined effect of the buncher RF fields and realistic quadrupole magnetic fields on the transverse emittances is approximately multiplicative. One can conclude that MEBT modifications are necessary.

The first step should be quadrupole design modifications to reduce the field non-linearities at large radii and edge fields. The options include increasing the quad aperture and/or length; replacing EM (some or all) with permanent-magnet quadrupoles (PMQ); or adjusting pole-tip shapes. We explored some options in [5]. Our PS PIC simulation results for a few MEBT configurations with the PS input distribution are summarized in Table 3.

Table 3: Parameter Changes vs. MEBT Configuration

C	B	Q	S	N/N_0	$\varepsilon_x/\varepsilon_{x0}$	$\varepsilon_y/\varepsilon_{y0}$	$\varepsilon_z/\varepsilon_{z0}$
p1	on	EM	on	0.968	3.08	2.32	1.37
p2	on	HE	*	0.979	1.92	1.24	1.26
p3	on	PMQ	on	0.983	2.56	2.32	1.29
p4	on	aEM	on	0.971	2.96	2.28	1.37

* Ideal HE steerers are on.

The cases in Table 3: p1 – real MEBT; p2 – ideal HE quads and ideal steerers (no coupling); p3 – PM quads; p4 – EM quads with alternative pole tips. From comparison with Table 2 (1 vs p1), one can see that emittances increase similarly for both input distributions, except that ε_y grows a bit more for the PS input. The RF buncher fields affect the PS input distribution stronger than the one from ParmteqM (2 vs p2). "Alternative" quads give only small improvements (p4 vs p1), but with PMQs (p3 vs p1) the improvements are more noticeable. Obviously, the MEBT design should be further optimized.

CONCLUSION

We explored beam dynamics in the MEBT for the new proton RFQ-based injector at LANSCE with CST Particle Studio particle-in-cell (PIC) 3D simulations to take into account effects of the large beam size and field overlaps. The CST-calculated fields of quarter-wave RF buncher cavities and of quadrupole magnets with steerers were applied. Two realistic initial beam distributions were used in our PIC runs. We found that for both distributions the beam transverse emittances increase significantly more than was predicted in the original MEBT design [2], which was based on the standard approach using envelope codes and Parmila simulations. One the other hand, the longitudinal emittance growth is lower than in [2]. Our explanation for these differences is that with the very large beam size in MEBT, which is required to further transfer the beam through a long transfer line to DTL, 3D field effects and field overlaps from adjacent elements become essential; they cannot be taken into account by only traditional beam dynamics codes. From this viewpoint, the considered RFQ MEBT is an important example where simulations with traditional codes are insufficient to correctly predict the beam dynamics.

The emittance growth is caused mainly by the magnetic fields of short EM quadrupoles. The buncher RF fields also contribute. We considered some possible modifications of the MEBT quads and showed that they help; in particular, using permanent-magnet quadrupoles improves the MEBT performance. However, further optimization is required.

ACKNOWLEDGMENT

The author would like to thank Y. Batygin, L. Rybarcyk, and D. Shchegolkov (LANL) for useful discussions.

REFERENCES

[1] R.W. Garnett *et al.*, "Status of the LANSCE front-end upgrade," in *Proc. NA-PAC13*, Pasadena, CA, USA, 2013, p. 327.

[2] C.M. Fortgang *et al.*, "A Specialized MEBT Design for the LANSCE H^+ RFQ Upgrade Project," in *Proc. NA-PAC13*, Pasadena, CA, USA, 2013, p. 670.

[3] Los Alamos Accelerator Code Group, laacg.lanl.gov

[4] CST Studio Suite, CST, www.cst.com

[5] S.S. Kurennoy, Tech notes AOT-AE: 17-009, 18-005; "Beam dynamics modeling of the proton RFQ MEBT with CST PS," LA-UR-18-23434, Los Alamos, USA, 2018.

[6] S.S. Kurennoy, "3D Effects in RFQ Accelerators," in *Proc. Linac14*, Geneva, Switzerland, 2014, p. 1077.